Preprint typeset using LaTeX style emulateapj v. 03/07/07

UNSTABLE GRB PHOTOSPHERES AND $E^{\pm}$ ANNIHILATION LINES

KUNIHITO IOKA[1], KOHTA MURASE[2], KENJI TOMA[1], SHIGEHIRO NAGATAKI[2], AND TAKASHI NAKAMURA[1]

ABSTRACT

We propose an emission mechanism of prompt gamma-ray bursts (GRBs) that can reproduce the observed non-thermal spectra with high radiative efficiencies, $> 50\%$. Internal dissipation below a photosphere can create a radiation-dominated thermal fireball. If $e^{\pm}$ pairs outnumber protons, radiative acceleration of $e^{\pm}$ pairs drives the two-stream instabilities between pairs and protons, leading to the "proton sedimentation" in the accelerating pair frame. Pairs are continuously shock heated by proton clumps, scattering the thermal photons into the broken power-law shape, with the non-thermal energy that is comparable to the proton kinetic energy, consistent with observations. Pair photospheres become unstable around the radius of the progenitor star where strong thermalization occurs, if parameters satisfy the observed spectral (Yonetoku) relation. Pair annihilation lines are predicted above continua, which could be verified by GLAST.

Subject headings: gamma rays: bursts — gamma rays: theory — radiation mechanism: non-thermal

1. INTRODUCTION AND SUMMARY

The emission mechanism of the prompt Gamma-ray bursts (GRBs) (the most luminous objects in the universe) is still enigmatic despite the recent progresses in the Swift era (Mészáros 2006; Zhang 2007). Main issues are (A) the efficiency problem (Ioka et al. 2006; Zhang et al. 2007; Toma et al. 2006) and (B) the cooling problem (Ghisellini, Celotti & Lazzati 2000; Mészáros & Rees 2000). The first problem (A) is that the GRB radiative efficiency, defined by the GRB energy divided by the total energy including the afterglow energy, is too high ($> 50\%$) to be produced by the internal shocks. Although the high efficiency may be achieved by a large dispersion in the Lorentz factor of the outflows (Beloborodov 2000; Kobayashi & Sari 2001), this would yield smaller correlation coefficient for the observed spectral correlations, such as Amati and Yonetoku relations (Amati 2006; Yonetoku et al. 2004), as far as the non-thermal (synchrotron or inverse Compton (IC)) processes determine the spectral peak energy. The recent Swift observations make the problem even worse since the early afterglow energy is smaller than expected, raising some of GRB efficiencies up to $> 90\%$. The second problem (B) is that the cooling time is much shorter than the dynamical time, making the low-energy spectral slope steeper than the observations.

Motivated by these problems, thermal photosphere models are proposed where the outflow energy is internally dissipated and thermalized inside the photosphere (Thompson 1994; Ghisellini & Celotti 1999; Mészáros & Rees 2000). These models have an advantage to stabilizing the peak energy, which is identified with the thermal peak (Thompson et al. 2007; Rees & Mészáros 2005). Thermal peaks may be actually associated with up to 30% of long GRBs (Ryde 2005).

However a simple photosphere model is not compatible with observations that most GRBs are highly non-thermal. This is one reason that excludes the original fireball model (Paczyński 1986; Goodman 1986). Although Comptonization of the thermal photons via magnetic reconnection and/or turbulence is invoked for non-thermal spectra (Thompson et al. 2007; Giannios & Spruit 2007), the heating mechanism of electrons is largely uncertain.

In this Letter we propose a possible scenario to make photospheres non-thermal. We show that radiatively driven instabilities[3] occur in a radiation-dominated photosphere if $e^{\pm}$ pairs outnumber protons.[4] Since radiation selectively pushes pairs rather than protons, the relative velocity between pairs and protons increases, driving the two-stream instability, possibly of the Weibel type (§ 3). This produces the small-scale inhomogeneity of the proton-to-pair ratio, that could grow up to proton clumps causing shocks with pairs. Shocked pairs scatter thermal photons into the observed non-thermal spectra with energy comparable to the proton kinetic energy, consistent with observations. The unstable pair photosphere may be common since the observations including the Yonetoku relation (Yonetoku et al. 2004) suggest that the instabilities occur around the radius of the progenitor star where strong thermalization occurs (§ 2). Our model employs the radiation-dominated fireball, solving (A) the efficiency problem, and naturally achieves the continuous heating of pairs, solving (B) the cooling problem (§ 4). Pair annihilation lines are predicted above continua, which could enable GLAST to verify the pair photosphere model (Murase & Ioka 2007) (§ 5). We use the unit $k_B = h = 1$ and $Q_x = Q/10^x$ in cgs units unless otherwise stated.

2. PAIR PHOTOSPHERE AND YONETOKU RELATION

Most opacity of the fireball photosphere can be provided by $e^{\pm}$ pairs (Rees & Mészáros 2005; Mészáros et al. 2002; Pe'er & Waxman 2004). The observed GRB spectrum, if extrapolated, has a significant fraction of energy above the pair production threshold (Lithwick & Sari 2001; Baring & Harding 1997). So more pairs can be produced than electrons associated with protons. (Pairs are $m_p/m_e \sim 2000$ times more abundant if they have the same energy as protons.) We assume that internal dissipation such as shocks produces pairs via non-thermal processes and create the pair photosphere.

The plasma and photons are subsequently thermalized by scatterings under the photosphere. Assuming that we identify the thermal peak $T_{obs} = \Gamma T$ with the peak energy of GRBs, we obtain the luminosity $L \sim 4\pi r^2 a T^4 c \Gamma^2$ and hence the comov-

[1] Department of Physics, Kyoto University, Kyoto 606-8502, Japan
[2] YITP, Kyoto University, Oiwake-cho, Kitashirakawa, Sakyo-ku, Kyoto, 606-8502, Japan

[3] Our instability is different from that in Waxman & Piran (1994).
[4] We only consider protons for baryons for simplicity.

ing size of the photosphere as

$$\ell_p \equiv r/\Gamma \sim 4\times10^8 L_{51}^{1/2} T_{obs,2}^{-2}\ \mathrm{cm}, \quad (1)$$

where $T_{obs,2} = T_{obs}/100\mathrm{keV}$ and Γ is the bulk Lorentz factor. The optical depth of the pair photosphere is $\tau_{\gamma e} \sim n_\pm \sigma_T \ell_p \sim 1$, which yields the comoving number density of pairs as

$$n_\pm \sim 3\times10^{15} L_{51}^{-1/2} T_{obs,2}^{2}\ \mathrm{cm}^{-3}. \quad (2)$$

Our model requires that pairs are accelerated by radiation, so that the radiation dominates the pair rest energy, $aT^4 > n_\pm m_e c^2$. We also require that protons are not accelerated by radiation exerted on the associated electrons which is $\sim (n_p/n_\pm) aT^4$ since we are considering $n_\pm \gg n_p$ and $\tau_{\gamma e} \sim n_\pm \sigma_T \ell_p \sim 1$, so that $(n_p/n_\pm) aT^4 < n_p m_p c^2$. With equations (1) and (2), these limit the photospheric radius as

$$1\times10^{11} T_{obs,2}^{-3/2} L_{51}^{5/8}\ \mathrm{cm} < r < 7\times10^{11} T_{obs,2}^{-3/2} L_{51}^{5/8}\ \mathrm{cm}. \quad (3)$$

If we insert the observed Yonetoku relation (Yonetoku et al. 2004),

$$T_{obs} \propto L^{1/2} \quad \text{(Yonetoku relation)} \quad (4)$$

into the above relation, we have very weak parameter dependence as $\propto L^{-1/8}$. Interestingly the radius in Eq.(3) is comparable to the Wolf-Rayet stellar radius ~ 2–$20 R_\odot$ (Cox 2000). Considering that the strong dissipation occurs within the progenitor star via interactions at the jet-star boundary (Zhang et al. 2004), most GRBs could satisfy our model assumptions. Pairs expand to the light speed within the expansion time $\sim \ell_p/c$ with the comoving acceleration

$$g \sim \frac{c}{\ell_p/c} \sim 2\times10^{12} L_{51}^{-1/2} T_{obs,2}^{2}\ \mathrm{cm/s}^2. \quad (5)$$

For later use we define the mean proton density $\bar{n}_p$, which satisfies $\bar{n}_p \ll n_\pm$ for the pair photosphere. In this Letter, we take $n_\pm/\bar{n}_p = 10^3$, $T_{obs} = 100$ keV, $L = 10^{51}\mathrm{erg/s}$ and $\Gamma = 10^3$ for fiducial parameters. The energy density ratio is then $aT^4 : \bar{n}_p m_p c^2 : n_\pm m_e c^2 \sim 1 : 0.4 : 0.2$.

3. WEIBEL INSTABILITY BETWEEN $E^\pm$ AND PROTONS

Radiation selectively pushes pairs rather than protons because the cross section for scattering is proportional to the inverse square of mass $\sigma_T \propto m^{-2}$. Then the relative velocity between pairs and protons must rise in the initial stage. Here Coulomb collisions between pairs and protons are usually negligible. Collisionless interactions are also absent if the magnetic fields are weak in the initial fireball.

Then the relative velocity between pairs and protons drives the two-stream instability, in particular, of the Weibel type (Weibel 1959). Let us first consider the linear stage of the Weibel instability. The initial distribution function of each component is given by $f_j(\mathbf{v}) = (m_j/2\pi T_j)^{3/2} e^{-m_j[v_x^2+(v_y-V_j)^2+v_z^2]/2T_j}$, where m_j is the mass, T_j is the temperature, and V_j is the relative velocity for each component with $j = e^+, e^-, p$. Initially the system is nonrelativistic. Linearizing the Vlasov-Maxwell equation, we obtain the dispersion relation of the pair proton plasma as

$$c^2k^2 = \omega^2 - \sum_j \omega_{pj}^2 + \sum_j \omega_{pj}^2 \frac{T_j + m_j V_j^2}{T_j}\left[1+\xi_j Z(\xi_j)\right], \quad (6)$$

where $\omega_{pj}^2 = 4\pi n_j q_j^2/m_j$ is the plasma frequency, $Z(\xi) = \pi^{-1/2}\int_{-\infty}^{\infty} dx (x-\xi)^{-1} e^{-x^2}$ is the plasma dispersion function, and $\xi_j = \omega/k(2T_j/m_j)^{1/2}$ (Davidson et al. 1972). Note that we are considering the Lorentz frame in which the linearized Vlasov-Maxwell equation is block-diagonal ($D_{xy} = 0$),

$$\sum_j \frac{\omega_{pj}^2}{\omega^2}\left[1+\xi_j Z(\xi_j)\right]\frac{m_j}{T_j}\frac{\omega}{k} V_j = 0. \quad (7)$$

In the initial stage the relative velocity is small, $m_j V_j^2 \ll T_j$, so that we may simplify equation (6) since $\xi_j \ll 1$. With $Z(\xi) \simeq i\pi^{1/2}$ for $\xi \ll 1$, we find to leading order

$$\omega \simeq i\left(\frac{2}{\pi}\right)^{1/2} |k| \frac{\sum_j \omega_{pj}^2 \frac{m_j V_j^2}{T_j} - c^2k^2}{\sum_j \omega_{pj}^2 \left(\frac{m_j}{T_j}\right)^{1/2}}. \quad (8)$$

Therefore the plasma is unstable ($\Im\omega > 0$) for $0 \le k^2 \le k_0^2$ where $k_0^2 = \sum_j \omega_{pj}^2 m_j V_j^2/c^2 T_j$. The maximum growth rate is

$$(\Im\omega)_{\max} \simeq \left(\frac{8}{27\pi}\right)^{1/2} \frac{\left[\sum_j \omega_{pj}^2 \frac{m_j V_j^2}{T_j}\right]^{3/2}}{\sum_j \omega_{pj}^2 \left(\frac{m_j c^2}{T_j}\right)^{1/2}} \quad (9)$$

for

$$k_{\max}^2 = \sum_j \frac{\omega_{pj}^2 m_j V_j^2}{3c^2 T_j} = k_0^2/3. \quad (10)$$

Equation (7) which characterizes our Lorentz frame is also reduced to

$$\sum_j \omega_{pj}^2 \frac{m_j}{T_j} V_j \propto \sum_j \frac{n_j}{T_j} V_j = 0. \quad (11)$$

Let us apply equation (9) to the fireball photosphere. Noting that (a) the pair density dominates the proton density, $n_+ \sim n_- \gg n_p$ (§ 2), (b) the relative velocity is initially smaller than the thermal one, $m_p V_p^2 < T_+ \sim T_- \sim T_p$, and (c) we have $-n_+ V_+ \sim n_- V_- \sim n_p V_p$ with equation (11) and the charge neutrality $\sum_j q_j n_j V_j = 0$, we find $\sum_j \omega_{pj}^2 m_j V_j^2/T_j \sim \omega_{pp}^2 m_p V_p^2/T$ and $\sum_j \omega_{pj}^2 (m_j c^2/T_j)^{1/2} \sim 2\omega_{pe}^2 (m_e c^2/T)^{1/2}$. Then the maximum growth rate in equation (9) is reduced to

$$(\Im\omega)_{\max} \sim \left(\frac{2}{27\pi}\right)^{1/2} \omega_{pp} \frac{\omega_{pp}^2}{\omega_{pe}^2} \left(\frac{m_p V_p^2}{m_e c^2}\right)^{1/2} \frac{m_p V_p^2}{T}$$
$$\sim 2\, n_{p,12}^{3/2} n_{-,15}^{-1} T_{-1}^{1/2} \left(\frac{m_p V_p^2}{T}\right)^{3/2} \mathrm{s}^{-1}, \quad (12)$$

where $T_{-1} = T/0.1\mathrm{keV}$ and we are assuming $V_p < (T/m_p)^{1/2}$. Note that the proton current direction is different from the pair one, and $|V_+| \sim |V_-| \ll |V_p|$ in the frame (11).

Comparing the growth rate $(\Im\omega)_{\max}$ in equation (12) with the acceleration rate $\sim g/V_p$ in equation (5), we find that the latter is larger $(\Im\omega)_{\max} < g/V_p$ under the condition $V_p < (T/m_p)^{1/2} \sim 1\times10^7 T_{-1}^{1/2}\mathrm{cm/s}$. This means that the relative velocity V_p overtakes the thermal one $\sim (T/m_p)^{1/2}$ before the Weibel instability develops.

Eventually the Weibel instability saturates in the velocity region $(T/m_p)^{1/2} < V_p < c$. Although no non-linear simulation exists so far for the proton streaming in pairs, the proton and pair flows will split into current filaments (cylindrical beam) that is bound by the self-generated magnetic fields

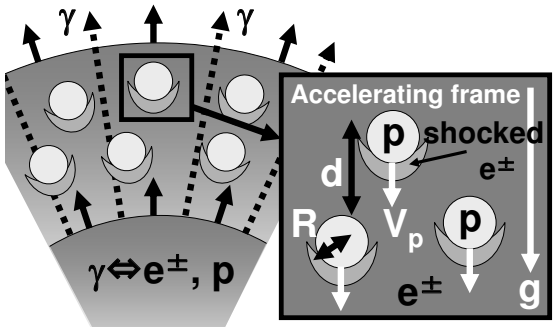

FIG. 1.— The schematic picture of the unstable GRB photosphere. Radiation selectively pushes pairs rather than protons, driving the two-stream instability between pairs and protons. This produces the small-scale inhomogeneity of the proton-to-pair ratio, that grows up to proton clumps causing shocks with pairs. In the accelerating pair frame, particles feel an effective gravity with the acceleration g in equation (5). Proton clumps fall down and merge, increasing their radii R, infall velocities V_p and vertical separation d.

(Silva et al. 2003; Nishikawa et al. 2003; Kato 2005). Since currents with the same (different) direction attract (expel) each other, protons effectively separate from pairs[5] and temporarily produce the small-scale inhomogeneity of the proton-to-pair ratio.

We note that each current can not separate completely if the relative velocity V_p is smaller than the thermal one $\sim (T/m_p)^{1/2}$ because the filament radius $\sim k_{\rm max}^{-1}$ in equation (10) is larger than the plasma skin depth, $r \sim k_{\rm max}^{-1} > c/\omega_{pp}$, and hence the current $I = \pi r^2 q n_p V_p$ exceeds the Alfvén current $I_A \equiv m_p c^2 V_p/q$ (the maximum current limited by the self-generated magnetic field) (Alfvén 1939), i.e., filaments must overlap to reduce the net current. This saturation is so-called the Alfvén limit (Kato 2005). This is not our case since $r < c/\omega_{pp}$ for $V_p > (T/m_p)^{1/2}$, i.e., in the particle limit (Kato 2005). Note also that the late evolution is mainly driven by protons since the kinetic energy of protons dominates that of pairs. The generated magnetic fields are weak $B^2/8\pi \lesssim n_p m_p V_p^2 \ll aT^4$ at this stage.

4. POSSIBLE SCENARIO FOR NON-THERMALIZATION

We have shown that protons will temporarily separate from pairs on the small-scale possibly via the Weibel instability. The subsequent scenario is very speculative but have attractive features that are worth pursuing. We consider in the frame comoving with pairs (that is almost the same as the frame in equation (7)). In this frame, particles feel an effective gravity with the acceleration g in equation (5). Unlike pairs that interact with radiation, protons fall down, which may lead to the "proton sedimentation" in the pair fireball (see Fig. 1).

Initially protons are trapped by magnetic fields on the scale of the filament radius. We model the inhomogeneity by the proton clumps with the filament size[6] ($R \sim c/\omega_{pp}$). Since a clump consists of many particles, the center-of-mass thermal motion is much less than the infall velocity. Also the acceleration time is comparable to the growth time of the instability, so that the clumps continue falling down and collide with other clumps within $t_m \sim R/\delta V_p \sim 2\times 10^{-6} n_{p,12}^{1/2} V_{p,7}^{-1}$ s where $\delta V_p \sim V_p$ is the relative velocity of clumps. Since the Larmor radius is comparable to the clump size, the fluid approximation begins to be valid. Then, we may apply the Stokes' law to estimate the terminal infall velocity as $V_p \propto n_p R^2$. Since the number density of clumps is $N_c \propto n_p^{-1} R^{-3}$ (mass conservation) and the cross section for the collision is $\sigma_c \propto R^2$, the merger timescale is

$$t_m \sim (N_c \sigma_c \delta V_p)^{-1} \propto R^{-1}. \tag{13}$$

This leads to runaway growth of clumps because the merger timescale is shorter for larger clumps.

After the terminal velocity exceeds the sonic speed of pairs $V_p > c_{s,\pm}$, we can not use the Stokes' law but instead the momentum balance. Since the pair mass colliding with a proton clump during Δt is $\Delta M \sim m_e n_\pm R^2 V_p \Delta t$, the momentum conservation gives the velocity change $\Delta V_p \sim V_p \Delta M/m_p n_p R^3$. Equating $\Delta V_p/\Delta t$ with the acceleration g, we find the terminal velocity as

$$V_p \sim \left(\frac{m_p n_p g R}{m_e n_\pm}\right)^{1/2}. \tag{14}$$

With $g \sim c^2/\ell_p$ in equation (5), the terminal velocity reaches the light speed $V_p \sim c$ when the ratio of clumps to the system size is $R/\ell_p \sim m_e n_\pm/m_p n_p < 1$. So the final separation between clumps in the vertical direction is about

$$d \sim \frac{n_p}{\bar{n}_p} R \sim \ell_p \frac{n_\pm m_e}{\bar{n}_p m_p}, \tag{15}$$

since the swept mass is $R^2 d\bar{n}_p \sim R^3 n_p$.

Collisionless shocks arise as the relative velocity between proton clumps and pairs approaches the light speed. Pairs are shock heated and accelerated to a power-law distribution $N(\gamma_\pm)d\gamma_\pm \propto \gamma_\pm^{-p} d\gamma_\pm$ for the pair Lorentz factor $\gamma_\pm \geq \gamma_m \sim 1$, where γ_m is the minimum Lorentz factor. Shocked pairs are pushed sideways and then again shocked by other clumps (see Fig. 1). The timescale between shocks is about $\sim d/c$ in equation (15), and interestingly this is comparable to the IC cooling timescale,

$$\mathcal{R} \equiv \frac{t_c}{d/c} \sim \frac{\gamma_\pm m_e c^2}{c\sigma_T U_\gamma \gamma_\pm^2}\frac{c}{d} \sim \frac{\bar{n}_p m_p c^2}{\gamma_\pm U_\gamma}, \tag{16}$$

for $\gamma_\pm \sim 1$ if the proton energy is comparable to the radiation energy $\bar{n}_p m_p c^2 \sim U_\gamma \equiv aT^4$ (as our parameters), where we use $\tau_{\gamma e} \sim n_\pm \sigma_T \ell_p \sim 1$ in the second equality. *Therefore the clumps automatically have the right separation for the continuous heating of pairs.* Since a photon is scattered by $\gamma_\pm \sim 1$ pairs once on average for $\tau_{\gamma e} \sim 1$, scattered photons have the energy density

$$\mathcal{R} U_\gamma \sim \bar{n}_p m_p c^2. \tag{17}$$

Thus, the non-thermal component has comparable energy to the proton kinetic energy, consistent with observations.

Neglecting multiple scatterings since $\tau_{\gamma e} \sim 1$, we may calculate the observed IC spectrum as (Sari & Esin 2001)

$$F_\nu = \begin{cases} (\nu/T_{obs}) F_{\nu,\rm max}, & \nu < T_{obs}, \\ (\nu/T_{obs})^{-p/2} F_{\nu,\rm max}, & T_{obs} < \nu, \end{cases} \tag{18}$$

that also peaks at the thermal peak $\nu \sim T_{obs}$ for $p > 2$ because $\gamma_m \sim 1$ (see Figure 2). The ratio of the IC peak flux to the thermal one is $F_{\nu,\rm max}/F_{\nu,\rm max}^{BB} \sim \bar{n}_p m_p c^2/U_\gamma$ (~ 1 for our parameters). At high frequencies $\nu > T_{obs}$, the IC spectrum has a cooling spectrum $\propto \nu^{-p/2}$ since the cooling is faster than the heating, $t_c < d/c$, for $\gamma_\pm > 1$. At low frequencies $\nu < T_{obs}$, the Rayleigh-Jeans spectrum $\propto \nu^2$ is modified to $\propto \nu$ by down-scatterings. Therefore the total (IC plus thermal) spectrum is roughly a broken power-law peaking at $\nu \sim T_{obs}$ and resembles the observed GRB spectrum although the low energy photon index is slightly harder.

[5] A small fraction of electrons that preserve the charge neutrality exists in the proton filament.

[6] Magnetic clumps are observed in the particle simulations, though not applicable to our pair proton case. (Chang, Spitkovsky & Arons 2007).

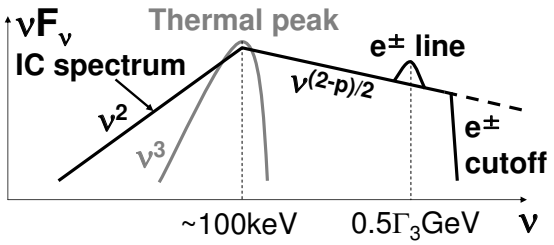

FIG. 2.— The schematic picture of the GRB spectrum in our unstable photosphere model. Shocked pairs scatter thermal photons into the observed broken power-law spectra with energy comparable to the proton kinetic energy, consistent with observations. The pair annihilation line is predicted above continua in the pair photosphere model, which is blueshifted to $\nu \sim 0.5\Gamma_3$ GeV and broadened by the order-of-unity distribution of the Lorentz factor on the photosphere. At higher energy, a spectral cutoff arises due to the pair creation. A closure relation exists between observable quantities of lines and cutoffs (Murase & Ioka 2007), which may be verified by GLAST.

5. PREDICTION OF $E^{\pm}$ ANNIHILATION LINES

We can prove that the pair photosphere accompanies the pair annihilation line that is detectable above the power-law continuum if $\gamma_{\pm} \sim 1$. Let us assume that the continuum exceeds the annihilation line, $n_{\gamma,c} > n_{\gamma,l}$, where $n_{\gamma,c}$ ($n_{\gamma,l}$) is the number density of continuum (line) photons at the line energy. On the pair photosphere, $n_{\pm}\sigma_T l \sim 1$, we have $n_{\gamma,l} \sim n_{\pm}$ because the pairs annihilate once on average in the dynamical time, $\dot{n}_{\pm}\ell_p/c \sim -n_{\pm}^2\sigma_T\ell_p \sim -n_{\pm}$ (Svensson 1987). Then the optical depth to the pair production is larger than unity,

$$\tau_{\gamma\gamma} \sim n_{\gamma,c}\sigma_T\ell_p > n_{\gamma,l}\sigma_T\ell_p \sim n_{\pm}\sigma_T\ell_p \sim 1, \qquad (19)$$

and hence the continuum photons create more pairs than the existing pairs. However this contradicts with the definition of the pair photosphere. Therefore the assumption $n_{\gamma,c} > n_{\gamma,l}$ is wrong and the annihilation line should stand out of the continuum. As is clear from the above proof, the line flux is comparable to the continuum one when pairs are created from the continuum photons.

The lines are blueshifted to $\nu \sim 0.5\Gamma_3$ GeV (Pe'er, Mészáros & Rees 2006) and broadened by the order-of-unity distribution of the Lorentz factor on the photosphere. At higher energy, a spectral cutoff arises due to the pair creation (Asano & Inoue 2007; Baring & Harding 1997; Lithwick & Sari 2001; Razzaque, Mészáros & Zhang 2004). A closure relation exists between observable quantities of lines and cutoffs for the pair photosphere (Murase & Ioka 2007), which may be verified by GLAST.

6. DISCUSSIONS

The Yonetoku relation (4) can be derived from equation (1) if the photosphere appears at the stellar radius $r \sim$ const., as suggested in § 2, and the outflow rate of slow mass satisfies $\dot{M}_s \propto \Gamma_s$ because the Lorentz factor after two mass collision is about $\Gamma \sim (L\Gamma_s/\dot{M}_s c^2)^{1/2} \propto L^{1/2}$. We can test $\Gamma \propto L^{1/2}$ since Γ is determined by the annihilation lines.

Our model predicts (a) (non-thermal energy) $\sim$ (proton energy) $\sim$ (afterglow energy) and hence thermal peaks may outstand for GRBs with $> 90\%$ efficiencies. (b) Low energy index that is comparable to the observed hardest one. Superpositions of pulses or incomplete thermalization may produce softer index. (c) Dim optical flashes from reverse shocks (Li et al. 2003), consistent with recent observations. (d) Polarization in the non-thermal component (except for the thermal peak) produced by IC scatterings. (e) High energy cosmic rays and neutrinos since protons might be also accelerated at shocks. Particle simulations with pairs and protons are needed to verify our model. Other plasma instabilities, such as the electrostatic two-stream instability or the drift-wave instability with the initial magnetic fields, may also generate the initial proton inhomogeneity.

We thank K. Asano and T. Kato for useful comments. This work is supported in part by Grant-in-Aid for the 21st Century COE "Center for Diversity and Universality in Physics" from the Ministry of Education, Culture, Sports, Science and Technology (MEXT) of Japan and by the Grant-in-Aid from the Ministry of Education, Culture, Sports, Science and Technology (MEXT) of Japan, No.18740147 (K.I.), No.19104006, No.19740139 (S.N.) and No.19540283, No.19047004 (T.N.).

REFERENCES

Alfvén, H. 1939, Phys. Rev., 55, 425
Amati, L. 2006, MNRAS, 372, 233
Asano, K., and Inoue, S. 2007, arXiv:0705.2910
Baring, M. G., & Harding, A. K. 1997, ApJ, 491, 663
Beloborodov, A. M. 2000, ApJ, 539, L25
Chang, P., Spitkovsky, A., and Arons, J. 2007, arXiv:0704.3832
Cox, A. N. 2000, Allen's Astrophysical Quantities (4th ed.; New York: AIP)
Davidson, R. C., Hammer, D. A., Haber, I., and Wagner, C. E. 1972, Phys. Fluids, 15, 317
Ghisellini, G., and Celotti, A. 1999, ApJ, 511, L93
Ghisellini, G., Celotti, A., and Lazzati, D. 2000, MNRAS, 313, L1
Giannios, D, and Spruit,H. C. 2007, A&A, 469, 1
Goodman, J. 1986, ApJ, 308, L47
Ioka, K., Toma, K., Yamazaki, R., and Nakamura, T. 2006, A&A, 458, 7
Kato, T. N. 2005, Phys. Plasmas., 12, 080705
Kobayashi, S., and Sari, R. 2001, ApJ, 551, 934
Li, Z., Dai, Z. G., Lu, T., and Song, L. M. 2003, ApJ, 599, 380
Lithwick, Y., & Sari, R. 2001, ApJ, 555, 540
Mészáros, P. 2006, Rep. Prog. Phys., 69, 2259
Mészáros, P., Ramirez-Ruiz, E., Rees, M. J., and Zhang, B. 2002, ApJ, 578, 812
Mészáros, P., and Rees, M. J. 2000, ApJ, 530, 292
Murase, K., and Ioka, K. 2007, submitted
Nishikawa, K.-I., et al. 2003, ApJ, 595, 555
Paczyński, B. 1986, ApJ, 308, L43
Pe'er, A., Mészáros, P., & Rees, M. J. 2006, ApJ, 642, 995
Pe'er, A., and Waxman, E. 2004, ApJ, 613, 448
Razzaque, S., Mészáros, P., and Zhang., B. 2004, ApJ, 613, 1072
Rees, M. J., and Mészáros, P. 2005, ApJ, 628, 847
Ryde, F. 2005, ApJ, 625, L95
Sari, R., and Esin, A. A. 2001, ApJ, 548, 787
Silva, L. O., et al. 2003, ApJ, 596, L121
Svensson, R. 1987, MNRAS, 227, 403
Thompson, C. 1994, MNRAS, 270, 480
Thompson, C., Mészáros, P., and Rees, M. J. 2007, ApJ, in press, astro-ph/0608282
Toma, K., Ioka, K., Yamazaki, R., and Nakamura, T. 2006, ApJ, 640, L139
Waxman, E., and Piran, T. 1994, ApJ, 433, L85
Weibel, E. S. 1959, Phys. Rev. Lett., 2, 83
Yonetoku, D., Murakami, T., Nakamura, T., Yamazaki, R., Inoue, A., and Ioka, K. 2004, ApJ, 609, 935
Zhang, B. 2007, Chinese J. Astron. Astrophys., 7, 1
Zhang, B., et al. 2007, ApJ, 655, 989
Zhang, W., Woosley, S. E., and Heger, A. 2004, ApJ, 608, 365